AD-A170 690 STUDIES OF CHAIN CONFORMATIONAL KINETICS IN POLY(DI-N-AKYLSILANES) BY SPE..(U) IBM ALMADEN RESEARCH CENTER SAN JOSE CA H KUZMANY ET AL. 07 AUG 86 TR-6 1/1

UNCLASSIFIED N00014-85-C-0056 F/G 7/3 NL

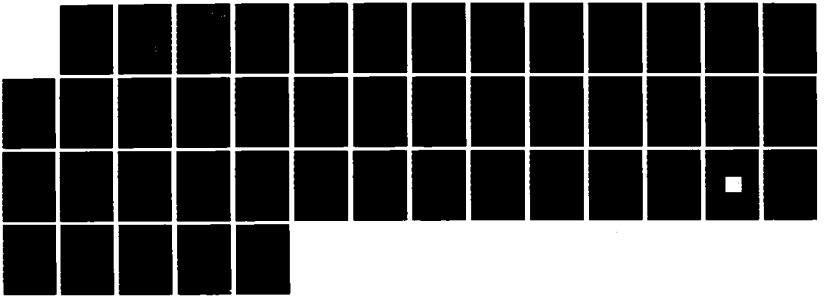

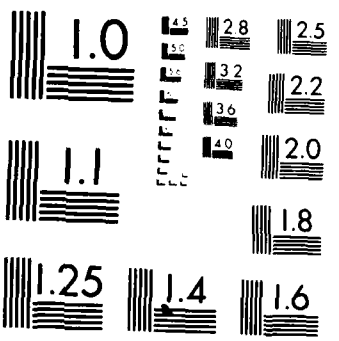

OFFICE OF NAVAL RESEARCH
CONTRACT N0014-85-C-0056
TASK NO. 631-850

"STUDIES OF CHAIN CONFORMATIONAL KINETICS IN POLY(DI-N-AKYLSILANES) BY SPECTROSCOPIC METHODS. 2. CONFORMATION AND PACKING OF POLY(DI-N-HEXYLSILANE)"

by
H. Kuzmany, J. F. Rabolt, B. L. Farmer, R. D. Miller

Submitted to Journal Chemical Physics

IBM Almaden Research Laboratory
650 Harry Road
San Jose, CA 95120-6099
August 7, 1986

SECURITY CLASSIFICATION OF THIS PAGE

REPORT DOCUMENTATION PAGE

1a REPORT SECURITY CLASSIFICATION	1b RESTRICTIVE MARKINGS
2a. SECURITY CLASSIFICATION AUTHORITY UNCLASSIFIED	3 DISTRIBUTION / AVAILABILITY OF REPORT DISTRIBUTION STATEMENT A Approved for public release; Distribution Unlimited
2b. DECLASSIFICATION / DOWNGRADING SCHEDULE	
4. PERFORMING ORGANIZATION REPORT NUMBER(S) TECHNICAL REPORT NO. 6	5. MONITORING ORGANIZATION REPORT NUMBER(S)
6a. NAME OF PERFORMING ORGANIZATION IBM RESEARCH 6b. OFFICE SYMBOL (If applicable)	7a. NAME OF MONITORING ORGANIZATION ONR
6c. ADDRESS (City, State, and ZIP Code) IBM ALMADEN RESEARCH LABORATORY 650 HARRY ROAD SAN JOSE, CA. 95120-6099	7b. ADDRESS (City, State, and ZIP Code) OFFICE OF NAVAL RESEARCH CHEMISTRY ARLINGTON, VA. 22217
8a. NAME OF FUNDING / SPONSORING ORGANIZATION ONR 8b. OFFICE SYMBOL (If applicable)	9. PROCUREMENT INSTRUMENT IDENTIFICATION NUMBER
8c. ADDRESS (City, State, and ZIP Code) OFFICE OF NAVAL RESEARCH(CHEMISTRY) 800 QUINCY STREET ARLINGTON, VA. 22217	10 SOURCE OF FUNDING NUMBERS PROGRAM ELEMENT NO: N0014-85 C-0056 / PROJECT NO / TASK NO. / WORK UNIT ACCESSION NO

11 TITLE (Include Security Classification) STUDIES OF CHAIN CONFORMATIONAL KINETICS IN POLY(DI-n-ALKYLSILANES) BY SPECTROSCOPIC METHODS. 2.CONFORMATION AND PACKING OF POLY(DI-n-HEXYLSILANE)

12 PERSONAL AUTHOR(S)
H. KUZMANY, J. F. RABOLT, B. L. FARMER, R. D. MILLER

13a. TYPE OF REPORT	13b. TIME COVERED	14. DATE OF REPORT (Year, Month, Day)	15. PAGE COUNT
PUBLICATION	FROM ____ TO ____	~~7-17~~-86 AUG. 7	27

16. SUPPLEMENTARY NOTATION
SUBMITTED TO J. CHEMICAL PHYSICS

17 COSATI CODES			18 SUBJECT TERMS (Continue on reverse if necessary and identify by block number)
FIELD	GROUP	SUB-GROUP	POLYSILANES, SOLID STATE CONFORMATIONS, THERMOCHROMISM

19. ABSTRACT (Continue on reverse if necessary and identify by block number)

ABSTRACT: Unoriented and highly oriented films of poly(di-n-hexylsilane) have been studied by Raman scattering, wide angle X-ray diffraction and optical absorption measurements. From a comparison of group theoretical predictions with those bands observed in the Raman experiments and from the X-ray layer line spacing in an oriented sample, a planar zig-zag conformation for the silicon backbone was deduced. X-ray reflections were suitable indexed by a monoclinic unit cell containing two molecules. Polarized Raman studies on uniaxially oriented samples also revealed that the hexyl side chains are not orthogonal to the silicon backbone but may be slightly titled in order to minimize intramolecular steric interactions.

20 DISTRIBUTION / AVAILABILITY OF ABSTRACT ☐ UNCLASSIFIED/UNLIMITED ☐ SAME AS RPT ☐ DTIC USERS	21. ABSTRACT SECURITY CLASSIFICATION
22a NAME OF RESPONSIBLE INDIVIDUAL	22b. TELEPHONE (Include Area Code) / 22c. OFFICE SYMBOL

STUDIES OF CHAIN CONFORMATIONAL KINETICS IN POLY(di-n-ALKYLSILANES) BY SPECTROSCOPIC METHODS 2. CONFORMATION AND PACKING OF POLY(di-n-HEXYLSILANE)

H. Kuzmany

Institut f. Festkorperphysik
University of Vienna
Vienna, Austria

and

J. F. Rabolt
B. L. Farmer*
R. D. Miller

IBM Almaden Research Center
650 Harry Road
San Jose, California 95120-6099 USA

STUDIES OF CHAIN CONFORMATIONAL KINETICS IN POLY(di-n-ALKYLSILANES) BY SPECTROSCOPIC METHODS 2. CONFORMATION AND PACKING OF POLY(di-n-HEXYLSILANE)

H. Kuzmany

Institut f. Festkorperphysik
University of Vienna
Vienna, Austria

and

J. F. Rabolt
B. L. Farmer*
R. D. Miller

IBM Almaden Research Center
650 Harry Road
San Jose, California 95120-6099 USA

ABSTRACT: Unoriented and highly oriented films of poly(di-n-hexylsilane) have been studied by Raman scattering, wide angle X-ray diffraction and optical absorption measurements. From a comparison of group theoretical predictions with those bands observed in the Raman experiments and from the X-ray layer line spacing from an oriented sample, a planar zig-zag conformation for the silicon backbone was deduced. X-ray reflections were suitably indexed by a monoclinic unit cell containing two molecules. Polarized Raman studies on uniaxially oriented samples also revealed that the hexyl side chains are not orthogonal to the silicon backbone but may be slightly tilted in order to minimize intramolecular steric interactions.

---

*Permanent Address: Department of Materials Science and Engineering, Washington State University, Pullman, Washington, 99164-2720.

INTRODUCTION

Physical properties of polymers which are directly related to their electronic structure, e.g., optical absorption, thermoelectricity, magnetic properties and conductivity, are attracting considerable interest in both basic and applied scientific research. Thus far most of this work has been performed on conjugated π-electron systems[1,2] but very recently a group of nonconjugated, σ-bonded polymers, the poly(di-n-alkylsilanes), were reported to exhibit interesting electronic and structural properties.[3,4] Many[3] of these polymers undergo an order-disorder phase transition slightly above room temperature which is accompanied by changes in their optical absorption and other spectroscopic properties. In poly(di-n-hexylsilane) (PDHS) this transition has been studied[4] by thermal measurements, wide angle X-ray diffraction (WAXD) and infrared spectroscopy. The optical absorption was observed to shift from 317 nm in the high temperature phase to 374 nm in the low temperature crystalline state. A preliminary study[4] of the Raman spectrum showed that a dramatic decrease in the scattering intensity accompanied the phase transition. The mechanism of this phase transition was identified as a melting of the side chains which drives the Si-backbone into a partially disordered state. However, except for theoretical studies[5] very little is known about the conformation of the polymer chain or the structure of the crystallographic unit cell.

This paper reports a detailed study of the structure and the phase transition of PDHS as obtained by optical measurements, Raman scattering and X-ray diffraction. Oriented films were shown to exhibit a strong anisotropy of the electronic transition moments in the crystalline state. Raman scattering in conjunction with WAXD measurements from these oriented films has provided information about the structure of the side chains and the backbone. In addition a strong enhancement of the Raman spectrum of PDHS has

been attributed to a preresonance scattering process with the shift of the optical absorption (resulting from the decrease in the length of all trans sequences along the backbone) responsible for the disappearance of the Raman spectrum at the phase transition.

A. Experimental Sample Preparation

Polymer samples of PDHS were prepared by condensation of dichloro di-n-hexylsilane in a solution of diglyme in toluene as described previously.[6] The polymer was precipitated by pouring the reaction mixture into isopropyl alcohol. After filtering, washing, and removing the solvent, a solid white polymer was obtained. The polymer was completely soluble in toluene and other organic solvents and was found to exhibit a bimodal molecular weight distribution. The material was fractionated by repeated precipitation with isopropyl alcohol until a clean fraction of high molecular weight ($\sim 2 \times 10^6$) was obtained. This fraction was used exclusively for the experiments described here.

Free standing films were obtained by casting a viscous solution of the polymer in toluene onto a glass substrate and pealing off the film after evaporation of the solvent. The films thus obtained (1-10μ) were transparent or slightly milky. Orientation of the films was accomplished by heating the substrate and polymer beyond the phase transition temperature and peeling the film from the substrate. This procedure had to be terminated before the recrystallization process started since films in the crystalline phase were not ductile. For the high temperature phase, draw ratios of 100% to 1000% could be obtained. The drawn films were completely clear and highly transparent. Samples for the resonance Raman experiments were prepared on fused quartz of 0.5 mm thickness.

Similarly, very thin films which were prepared by spinning the solution of the polymer on a NaCl substrate were used to obtain optical spectra at various temperatures.

B. Characterization

Raman spectra were recorded using a Jobin-Yvon HG-2S double monochromator with holographic gratings and a spatial filter to enhance stray light rejection. The spectral resolution was between 1.5 and 3 cm^{-1}. Spectra were excited by irradiation of the samples with various lines from an argon or krypton ion laser with powers of between 40 and 80 mW. A 90° scattering geometry with the incident laser beam parallel to the X-direction and the scattered light parallel to the Z-direction was used. In all experiments the scattered light was scrambled before entering the monochromator in order to take into account the anisotropic scattering properties of holographic gratings. The scattered light was detected by a cooled RCA 31034A-02 photomultiplier tube using standard photon counting electronics. All data were collected and processed digitally by a Nicolet 1180 Data System. Variable temperature measurements were made in a Harney-Miller cell at temperatures in the range -40°C to +40°C.

Room temperature X-ray powder diffraction data were obtained between 5 and 45 degrees 2θ in 0.05 degree increments using an automated diffractometer in step-scan mode. Data from powders and oriented films were obtained at room and elevated temperatures using an evacuated flat plate camera (Warhus) with a nominal sample to film distance of 5 cm. X-ray fiber patterns were obtained from an oriented film specimen using a cylindrical camera with a diameter of 57.3 mm. In every case, nickel-filtered CuK_α (λ=1.54Å) radiation was used.

RESULTS

A. Raman Studies of Oriented PDHS Films

Raman results on a highly drawn film of PDHS, obtained according to the scattering geometry depicted in Figure 1, are shown in Figure 2, where they are compared with that (Figure 2A) obtained from an unoriented sample. The notation for each Raman spectrum describing its scattering geometry, direction of incident polarization and position of analyzer is due to Porto[7] and is used to label the spectra shown in Figure 2. The scattering designation is of the form A(BC)D, where A and D are the propagation directions of the incident (A) and scattered (D) radiation, while B and C refer to the polarization direction of the incident (B) and analyzed (C) radiation, respectively. Although the spectrum of the unoriented sample was obtained at room temperature, the spectra of the oriented film were recorded at -40°C. Thus the band intensities of spectrum 2A should not be directly compared to those of Figures 2B, C and D and are only included for reference.

The observed bands, listed in Table I, can be divided into three groups. Bands found in the region between 1040 cm^{-1} and 1500 cm^{-1} can be assigned to localized motions of the hexyl side chains, while those observed below 700 cm^{-1} are quite intense and originate from vibrations of the silicon backbone, at times coupled with delocalized motion of the side chain. These latter bands are, by far, the most intense since a vibration of the backbone causes a large change in the electron cloud (or polarizability) which is required for Raman intensity.

The final part of the spectrum between 700-1040 cm^{-1} is the most puzzling. Although it contains many bands, their assignment is not straightforward. It is, however, quite remarkable that most of the bands in this region are doublets, some examples of which are shown in Figure 3. This suggests that the origin of these bands arises from

vibrations of the hexyl groups with the splittings resulting from crystal field interactions between adjacent side chains. It is also not possible to rule out the presence of a small amount of a second structure.

In order to elucidate the assignment of the bands in the low frequency region, Raman measurements were also obtained from an isotopically enriched sample of PDHS in which the two carbon atoms adjacent to the silicon backbone were replaced by ^{13}C. Spectra of PDHS and PDHS – ^{13}C are shown in Figure 4. A noticeable shift is observed for the band at 689.5 cm^{-1} which is found at 680 cm^{-1} in the isotopically enriched sample. This clearly indicates that this band can be attributed to vibration of the Si-C bond. In addition, a band located at 482 cm^{-1} appears in the spectrum of ^{13}C enriched PDHS. This band does not appear to originate from isotopic substitution since it also appears in the virgin PDHS (see Figure 2(A)). However after heating above the transition point, the 482 cm^{-1} band disappears (see bottom panel of Figure 9) and thus appears to be thermal history dependent. Its origin is, as yet, unclear but evidence suggests that it can be attributed to the presence of a second non-trans conformation of the Si backbone. This conjecture is further reinforced by the observation that whenever the 482 cm^{-1} band is absent, that at 494 cm^{-1} gains a factor of two in intensity suggesting that there is a conversion of one conformer into the other after thermal treatment. In general, no other bands in the region below 750 cm^{-1} in the Raman spectrum of the isotopically substituted sample were observed to shift.

With respect to relative scattering intensities, the X(YY)Z spectrum is much stronger than the spectra for the other orientations. However, there are still several lines which exhibit a larger scattering intensity for the X(ZY)Z or X(ZX)Z scattering geometry. For the purpose of demonstration these bands are marked with a dashed line

in Figure 2. The very strong anisotropic scattering intensities for modes of the silicon backbone are a good indication of the high degree of orientation in the sample. In Figure 5 the polarization dependence[8] of the Raman intensities of the side chains is especially demonstrated for the lines at 1039 cm^{-1} (#18), 1059 cm^{-1} (#19) and 1297 cm^{-1} (#24). In this figure the scattering intensities for the various orientations are directly comparable. The vibrational modes corresponding to these three lines definitely correspond to different Raman tensor components. Since the latter two of these are assignable to vibrations of the n-hexyl side chain, their anisotropic scattering properties reflect the orientation of the side chain relative to the draw direction. This will be discussed in a later section.

Considerable polarization anisotropy was also observed in the CH stretching region as shown in Figure 6, where it is again compared to the spectrum of an unoriented powder. The overall complexity[9] of these bands can be attributed to the presence of both CH_3 and CH_2 contributions, as well as to the fact that not all the bonds of the n-hexyl side chain are trans planar due to the packing restrictions imposed by the chemical structure having two side chains attached to each silicon backbone atom. A more detailed discussion of the side chain packing constraints will follow in a later section.

B. X-ray Diffraction

The powder diffractometer scan of PDHS shows nearly thirty reflections in the angle range from 5 to 45 degrees 2θ. The d-spacings obtained from the diffractometer were considered to be more reliable than the values obtained from film measurements, and were therefore the values used for subsequent indexing and unit cell determination. The d-spacings measured from flat plate powder and fiber patterns and from cylindrical camera fiber patterns agreed with diffractometer values within about 2 percent.

In spite of the unusually large number of reflections (for a polymer), it was necessary to obtain fiber diffraction patterns from an oriented specimen before it was possible to index the reflections and determine a unit cell. The fiber patterns, an example of which is shown in Figure 7, were equally remarkable in their abundance of reflections, containing 25 hk0 and 16 hk1 reflections. D-spacings down to about 1.5Å remained sharp, indicating a very small amount of thermal disordering in the crystalline array at room temperature. The layer line spacing, indicative of the repeat distance along the fiber axis, was measured from three separate cylindrical-camera fiber patterns. The value of 4.07Å thus obtained indicates that the silicon backbone of the PDHS chain is in a planar zig-zag (all trans) conformation. If the Si-Si bond length is taken as the customary 2.35Å, the Si-Si-Si bond angle must be 120 degrees. While this value is perhaps higher than one might expect, it is not unreasonable considering the severe steric crowding of the hexyl side groups in this polymer.

In striking contrast to the large number of reflections observed at room temperature, at 60°C only a single sharp reflection remained at 13.5Å, accompanied by an amorphous halo at about 4.6Å. This reflection was comparable or somewhat stronger in intensity to the very strong reflection observed at room temperature. It should be noted that elevated temperature data could only be obtained using the flat plate camera (since the other diffraction equipment was not equipped for heating) and therefore the 13.5Å value could be subject to film reading inaccuracy and any change in the sample to film distance upon heating. The reflection, however, unmistakably occurs at smaller angles than the 11.8Å room temperature reflection.

C. Temperature Induced Phase Transition

Raman scattering and UV-Visible absorption experiments at various temperatures between 18°C and 43°C were used to study the temperature dependence of the phase transition. Figure 8 shows the UV-Visible absorption spectrum between 290 nm and 400 nm for a thin film on a NaCl substrate. This result is similar to that observed previously for isothermal heating of a quenched sample.[4]

Figure 9 shows the change of the Raman spectrum with increasing temperature and its recovery after lowering the temperature back to 17°C. Although the temperatures indicated in the figure are readings taken from the thermocouple, the real temperature in the sample could be larger by 3-5° due to laser heating. The figure shows the continuous decrease of scattering intensities with increasing temperature. The dramatic decrease in intensity can be attributed to a preresonance scattering process[10,11] as illustrated in Figure 10 where the Raman spectrum of PDHS has been recorded using three different excitation wavelengths. In all cases, the Raman intensity has been corrected for the ν^4 variation (since the spectra do represent a scattering process) thus normalizing all the spectra shown in Figure 10. It is quite clear that even after this normalization, the spectrum recorded with 4579Å excitation is, by far, the most intense, suggesting that resonance enhancement of the band intensities has occurred. The origin of this enhancement is thought to arise from the UV-Visible absorption at 374 nm with a long wavelength tail which extends into the visible. When excitation of the Raman spectrum occurs using the 457.9 nm, 488.0 nm or 514.5 nm laser lines, the scattering cross-section of the Si backbone and Si-C vibrations are enhanced and hence, they appear with a large intensity. Upon heating above 41°C, as shown previously, the UV-Visible absorption shifts to 317 nm and this preresonance condition no longer exists. Thus, the Raman band

intensities are no longer enhanced, giving rise to the broad weak spectrum depicted in Figure 9 (at 39°C).

It should be mentioned that using a higher laser power for the excitation of the spectra in similar experiments resulted in the generation of a strong luminescence background. This most likely results from serious radiation damage occurring in the sample. In the case of Figure 9, however, the spectrum recovers to its full relative intensity if the temperature is lowered back to 17°C as demonstrated by the spectrum in the lower panel. This rules out the fact that any serious sample damage has occurred during the temperature cycle.

In order to elucidate details about the temperature dependence of the phase transition and to see to which extent not only the peak intensities of the Raman bands but also their integrated intensities decrease, the latter are plotted in Figure 11 for the two bands at 689 cm^{-1} and 1450 cm^{-1}, respectively, as a function of the temperature. Integration was performed between 620 cm^{-1} and 760 cm^{-1} for the 689 cm^{-1} band and between 1410 cm^{-1} and 1500 cm^{-1} for that at 1450 cm^{-1}. Figure 11 illustrates a decrease of integrated intensities by more than one order of magnitude (10X) for the band at 689 cm^{-1} and by about a factor of 3 for the band at 1450 cm^{-1}. The intensity decrease starts immediately with the change of temperature but occurs slowly at first, then speeds up after a certain temperature is reached. Then, within about a 7° range, the phase transition occurs. Finally the ratio of the integrated intensities reaches a constant but finite value. As observed in the results of Figure 11 this value is larger for the band in the 1450 cm^{-1} region than for that at 689 cm^{-1} (see Table I). Reducing the temperature yields a strong hysteresis of about 7° but finally the full integrated intensities of the original spectra are regained. As discussed previously the band at 482 cm^{-1} is considerably reduced in

intensity after the sample is heated above its transition point while that at 494 cm^{-1} gains approximately a factor of two in intensity.

DISCUSSION

A. Structure of the Unit Cell

From an analysis of the Raman and WAXD measurements on oriented PDHS, information on the molecular and crystal structure of PDHS can be deduced.

As a starting point for interpreting the X-ray data, it was assumed that the unit cell was metrically monoclinic, *i.e.*, that two of the unit cell vectors were perpendicular to the cell vector in the chain direction (taken as c=4.07Å), but have an arbitrary angle to one another. All reflections in the powder diffractometer scan having d-spacings greater than 4.07Å must be of type hk0. Indeed, each such reflection did have a corresponding reflection on the zero layer of the fiber pattern.

Using a least-squares procedure to find the best fit between observed and calculated diffraction angles, it was possible to index all zero layer reflections observed in the diffractometer scan. The indices and calculated and observed d-spacings are presented in Table II. The average discrepancy in d values is 0.015Å and in diffraction angle 0.034 degrees, a value which is comparable to the experimental error, considering the step increment of 0.05 degrees used to take the data. The unit cell was found to have dimensions a=13.75Å, b=21.82Å, and γ=88.0 degrees. Since only hk0 data were used in this determination, these values may only represent the projections of the true cell parameters onto a plane perpendicular to the chain axis. Because the large unit cell dimensions result in a virtual continuum of potential reflections at d-spacings less than about 4.0Å (approximately one every 0.1Å), and since all upper layer reflections have such d-spacings, relaxing the requirement of a monoclinic system could not be justified.

Further refinement of the unit cell must await comparisons between observed and calculated intensities in order to ascertain which of the continuum of reflections will have observable intensities.

In order to be certain that indeed a monoclinic system was required, the least-squares procedure was attempted while holding the γ angle (between the a and b axes) fixed at 90.0 degrees. The best agreement between calculated and observed d-spacings gave 0.044Å average discrepancy, and 0.142 degree average discrepancy in diffraction angle. Considering the five-fold worsening in agreement, it can be stated with reasonable confidence that an orthorhombic unit cell is not likely.

The unit cell appears to be consistent with a reasonable packing mode for the PDHS chains. In the all-trans conformation, the molecules when drawn to approximate scale and allowing for typical atomic radii, are roughly rectangular in cross-section with dimensions 7Å by 19Å. With two molecules passing through each unit cell. The distance between silane backbones would be roughly 12Å, a value consistent with the strongest observed reflection at 11.8Å. Since this reflection (shifted to 13.5Å) is also the only one remaining in the diffraction pattern above the transition temperature, it might be supposed that the transition involves wholesale disordering of the hexyl side chain packing, but leaves the polymer backbones in approximately their same, nearly hexagonal packing arrangement as at room temperature.

As can be seen in Figure 7, there was a relatively strong diffraction maximum at about 13.8Å (just inside the very intense 11.8Å arcs) which maintained its nearly circular uniformity. While this reflection could be indexed by the proposed unit cell, this maximum probably corresponds to scattering from less ordered regions of the specimen, perhaps having the same origin as the observed Raman doublets noted earlier. Omission

of this reflection from the indexing procedure did not lead to better alternative unit cells for the polymer.

B. Conformation of Skeletal Backbone

Because of the large anisotropic scattering properties of oriented materials, Raman studies can be used to establish the correct molecular conformation when several structures are possible. In order to apply this analysis to PDHS, the backbone and the side chain will be considered independently.

In the region below 750 cm^{-1}, bands attributable to the nonlocalized vibrations of the backbone and those coupled with side chain vibrations are found. Band assignments can be made from studies of model linear and cyclosilanes[12-14] and their deuterated analogues which have appeared in the literature. The strong Raman band (Figure 2a) at 689 cm^{-1} which shifts to 679 cm^{-1} due to ^{13}C isotopic enrichment of the atom adjacent to the silane backbone can be assigned to symmetric stretching of the Si-C bonds. Its asymmetric counterpart is observed as a strong band at 673 cm^{-1} in the IR which shifts to 660 cm^{-1} upon isotopic substitution. Assignment of the silane backbone modes is a bit more difficult but recent studies of linear octamethyltrisilane by Hassler[14] does provide significant guidance. The strong Raman band at 372 cm^{-1} is assigned to the ν_s(Si-Si) stretching vibration while th weak band at 458 cm^{-1} can be attributed to the asymmetric Si-Si backbone stretch, ν_{as}(Si-Si). The remaining medium bands found at 467 and 494 cm^{-1} in samples previously heated above their 41°C transition and brought back to room temperature might result from the presence of a second non-trans conformer. More about this possibility will be discussed in a later section. A list of band assignments is contained in Table III.

As can be seen in Figures 2 and 6, the anisotropic scattering properties of a uniaxially oriented film are quite evident. The selection of the polarized Raman experiments shown in Figures 2B, C and D and 6 was designed to pick out vibrational modes belonging to each of the Raman active symmetry species through knowledge of the chain orientation relative to the filament axis, the factor group symmetry and the Raman scattering activities. With the unequivocal determination by WAXD that the backbone of PDHS was planar zig zag, a symmetry analysis of this conformation was undertaken. Raman scattering activities have been worked out by Snyder[15] for partially oriented systems in which a unique axis of the point group (by virtue of its being an axis of rotation or perpendicular to a reflection plane) lies parallel to the orientation direction. Similar expressions have been worked out by Schlotter and Rabolt[16] for the case when this unique axis is perpendicular to the direction of orientation.

For a planar zig zag backbone, the analysis by Snyder[15] can be used to determine the Raman scattering activities resulting from each experimental geometry. For the planar zig zag case, the factor group of the line group is isomorphic to the D_{2h} point group, exactly analogous to the symmetry analysis for polyethylene. The predictions for the experiments listed in Figures 2 and 6 are shown in Table IV.

As can be seen, the X(YY)Z experiment should select out those vibrational modes belonging to the A_g or totally symmetric symmetry species. Inspection of Figure 2B reveals four intense bands below 700 cm^{-1} located at 372, 467, 494 and 689 cm^{-1}. The 372 cm^{-1} band has been assigned to the ν_s(Si-Si) stretching vibration while the intense 689 cm^{-1} is most assuredly the ν_s(Si-C) stretch which was assigned based on Raman studies of isotopically enriched PDHS (see Table III). The origin of the two remaining features at 467 and 482 cm^{-1} is somewhat puzzling. Neither appears to be associated with

vibrational motion of the side chain since neither was observed to shift in the spectrum of isotopically substituted PDHS. The presence of these bands could possibly be attributable to a population of non-trans conformers whose Si-Si stretching vibrations occur in this region. Interestingly, the Raman spectrum of poly(di-n-tetradecylsilane) contains two strong bands in this region and preliminary data[17] suggest that it crystallizes with a non planar backbone possibly due to the length of the n-alkyl side chains. Certainly the polarization properties of these two low frequency bands are what would be expected for Raman active vibrations of a polymer backbone. In addition, it should also be pointed out that there has been a suggestion of a second phase from the UV-Visible spectrum,[3] Raman studies as a function of thermal history (presented here and discussed earlier), some recent results obtained from PDHS subjected to high pressure (~50 kbar),[18] and X-ray diffraction which shows the presence of strong amorphous scattering at room temperature.

According to the group theoretical analysis, the A_g bands will also be present in the X(ZX)Z spectrum shown in Figure 2D but will have different intensity since different components of the polarizability tensor will contribute. In addition, bands belonging to B_{1g} symmetry are also expected to occur in the X(ZX)Z spectrum but as shown in Figure 2D no such bands can be definitely identified.

At this point it is important to realize that some residual band intensity remaining in each of the spectra of Figure 2 could be attributable to a lack of complete molecular orientation and/or a slight misalignment of the sample in the beam. The former contribution can for the most part be ruled out since the WAXD pattern of oriented PDHS (Figure 7) was highly arced, indicative of very-highly oriented material. The result of sample misorientation in the beam can be assessed upon realization that, for the planar

zig zag conformational model of the backbone considered, the X(YX)Z and the X(ZY)Z measurements should give identical spectra. This then provides a criterion by which sample alignment can be measured. In the present study, relative band intensities in the X(YX)Z and X(ZY)Z experiments disagreed slightly, indicating that a tilt of ~10° had occurred during the measurements. This together with the presence of oriented but amorphous PDHS accounts for the residual intensity which is observed in these polarized Raman spectra.

As indicated in Table IV, bands of either B_{2g} or B_{3g} symmetry are expected to appear in the X(ZY)Z spectrum. Inspection of Figure 2C reveals that only the ν_a(Si-Si) band located at 458 cm^{-1} can be definitely assigned to the B_{2g} or B_{3g} symmetry species. No other backbone vibrations are expected and hence the residual intensity of the A_g modes obviously results from sample misalignment as indicated earlier.

C. Structure of the n-hexyl Side Chains

1. Orientation relative to the silane backbone. A discussion of the bands assigned to the n-hexyl side chains requires a symmetry analysis different from that used for the backbone. In this case, the main axis of symmetry (the n-hexyl side chain axis) is oriented at an angle relative to the orientation direction of the backbone and the expressions developed by Schlotter and Rabolt[16] must be used. As a starting point, a planar zig zag side chain normal to the plane of the silane backbone will be assumed to simplify the analysis. This idealized structure can still be discussed in terms of D_{2h} local symmetry, remembering that the predictions for each scattering geometry will be altered from those of the silane backbone. The purpose of discussing these band assignments according to local symmetry is that it then allows comparison with similar vibrational modes in short chain n-alkanes and polyethylene[8] listed in Table V. If the molecular z axis is coincident

with the axis of the n-hexyl side chain then it can be shown[16] that the following experiments will yield:

X(YY)Z	→	A_g
X(YX)Z	→	$B_{1g} + B_{2g}$
X(ZY)Z	→	$B_{1g} + B_{2g}$
X(ZX)Z	→	$A_{1g} + B_{3g}$

Inspection of Figure 2B, C and D shows the presence of a fair number of weak to medium bands above 1000 cm^{-1} which show significant intensity variations depending on the specific polarization experiment. As is shown in Table V, a number of these bands coincide with those found in n-alkanes and polyethylene and can thus be easily assigned. A more significant observation can be made by comparing the intensity variations of the *1059, 1175, 1295 and 1461 cm^{-1} bands in Figure 2B, C and D with those of their skeletal* backbone analogues $\leq$700 cm^{-1}. The intensities of the 372, 494 and 689 cm^{-1} backbone bands decrease significantly in going from Figure 2B to Figure 2D whereas the 1175 cm^{-1} side chain vibration has its intensity diminished by 30%. In a number of similar instances, it was observed that the vibrations of the side chain do not undergo the intensity changes (compared to those of the backbone) that would be expected from the polarized Raman experiments shown in Figure 2. This then suggests that the simplified model with the n-hexyl side chains normal to the axis of the silicon backbone is incorrect. This is further supported by consideration of the interatomic distances which would be necessary for an orthogonal structure. As shown in Figure 12 which contains a schematic diagram of two adjacent di-n-hexylsilane units, the two hydrogen atoms labelled 122 and 221 approach each other at unrealistically small distances (0.46 - 0.60Å depending on the specific choice of bond distances and angles). As a consequence, one can only conclude

that the side chains are not orthogonal to the silane backbone as confirmed by the polarized Raman measurements. Thus a rotation about the bond joining the silane backbone and the hexyl side chain must occur to relieve the intramolecular steric crowding. Detailed conformational energy calculations, currently in progress,[19] indicate that such a rotation is energetically favorable. Results will be published in the near future.

2. CH stretching region. A considerable amount of information about inter- and intramolecular order can be obtained from a study of the CH stretching region. Polarized Raman measurements of the CH stretching region of PDHS are shown in Figure 6 where they are compared with that obtained from an unoriented powder sample. The spectrum of the unoriented specimen is much richer (containing many broad overlapping bands) than that observed for long chain n-alkanes or polyethylene. The number of observed bands is understandable by comparison to that found for solid n-hexane, in which case no fewer than seven distinct bands, some having weak shoulders, can be found. Snyder et al.,[20] have shown that a minimum of five fundamental vibrations of the CH_2 and CH_3 groups are expected in addition to various weaker bands due to overtones of the CH_2 bending vibrations. As seen in the polarized Raman measurements, some simplification occurs due to the polarized character of certain CH stretching modes. The X(YX)Z spectrum is characterized by a single intense, highly polarized band located at 2885 cm^{-1} which is attributable to the asymmetric CH_2 stretch, $\nu_{as}(CH_2)$. The bandwidth and intensity of this vibration has been shown to be a very sensitive indicator of intermolecular order. Its sharpness in PDHS is thus indicative of the close packed n-hexyl side chains which exists at room temperature. The strong symmetric CH_2 stretching vibration is observed at 2846 cm^{-1} in the unoriented specimen and in the X(YY)Z scattering geometry consistent with its assignment to the A_g symmetry species.

The intensity of the 2885 cm^{-1} band relative to the 2846 cm^{-1} is indicative of the symmetry of the local CH_2 environment and has been used to determine the unit cell structure of n-alkanes.[20] In the case of PDHS, this intensity ratio is more characteristic of an orthorhombic subcell structure for the n-hexyl side chains. The presence of a 1415 cm^{-1} band in the CH_2 bending region is further evidence for such a structure.

Some of the other highly polarized bands shown in Figure 6, e.g., those at 2957 and 2870 cm^{-1} are due to vibrations of the methyl groups. Their moderate to strong intensity is due to the relatively high concentration of CH_3 groups (1:5) compared to CH_2 groups.

An additional factor which may account for the complexity of the CH stretching region is due to the orientation of the side chains relative to the silane backbone. As discussed previously, rotation about the Si-C and adjacent C-C bonds to relieve the steric hindrance of adjacent n-hexyl side chains will position two or more CH_2 groups in a non trans conformation. This will give rise to perturbed CH stretching vibrations which occur at slightly different frequencies adding to the already complex CH stretching region which results from all trans CH_2 groups.

CONCLUSIONS

The conformation and packing of PDHS chains has been investigated by wide angle X-ray diffraction, Raman scattering and UV-Visible absorption measurements at both room temperature and above its order-disorder phase transition (41°C). Raman band assignments were made based on spectroscopic studies of both protonated PDHS and an isotopically enriched analogue. Frequency shifts observed in the Raman spectrum of the latter allow the identification of those bands which could be attributed to vibrational motions of the backbone coupled to the side chains.

Studies of highly oriented films by WAXD revealed that the conformation of the silicon backbone is planar zig-zag at room temperature. In addition, the 41 observed X-ray reflections were suitably indexed by a monoclinic unit cell containing two molecules. Polarized Raman measurements on the identical uniaxially oriented sample support the existence of a planar zig-zag conformation. They also suggest the presence of a small amount of a second nonplanar conformer, perhaps attributable to the noncrystalline component.

Additionally, Raman studies of the n-hexyl side chains concluded that they are not oriented normal to the backbone but are slightly tilted to minimize intramolecular steric interactions. The exact nature of bond rotations needed to achieve this tilt is the subject of conformational energy calculations presently in progress.

ACKNOWLEDGMENT

This work is dedicated to Professor K. Komarek in honor of the 60th anniversary of this birthday. One of the authors (H.K.) acknowledges IBM-Austria for financial support for a sabbatical visit to IBM San Jose. He would also like to acknowledge Dr. Karpfen for many valuable discussions. R.D.M. acknowledges partial support for this work by the Office of Naval Research.

Table I

Observed Raman Bands of PDHS

No.	Frequency (cm^{-1})	I_{YY}	I_{YX}	I_{ZY}	I_{ZX}
1	336	16	6	2	3
2	372	244	42	9	2
3	421	---	3	3	2
4	458	16	27	16	3
5	467	120	20	5	1
6	482	4	---	---	1
7	494	212	51	20	4
8	662	24	5	1	---
9	689.5	953	110	41	12
10	727	40	8	4	6
11	754	24	6	---	---
12	835	30	7	2	1
13	874	2	---	---	---
14	890	3	4	5	10
15	913	3	---	---	---
16	943	38	7	2	1
17	998	16	5	3	3
18	1039	26	4	2	1
19	1059	0	6	5	11
20	1103	36	9	4	5
21	1155	2	---	---	---
22	1175	124	24	10	13
23	1244	26	3	1	2
24	1297	6	25	13	7
25	1414	8	2	1	2
26	1443	18	6	3	2
27	1453	24	10	7	11
28	1461	5	5	3	11
29	2846	13	2		6
30	2860	24	5		8
31	2870	24	---		14
32	2	26	16		16
33	2895	23	6		6
34	2925	12	4		10
35	2957	4	4		10

Table II

Wide Angle X-ray Diffraction Data for Oriented PDHS

hkl	d_{calc}	d_{obs}	I_{rel}
100	13.74	13.80+	21
110	11.81	11.81	100
120	8.7	8.9*	5
030	7.27	7.35	9
200	6.87	6.84	10
210	6.62	6.58	22
220	5.91	5.94	43
040	5.45	5.47	25
310	4.51	4.51	37
320	4.28	4.28	8
$1\bar{5}0$	4.12	4.11	5
330	3.94	3.97	8
021, $1\bar{1}1$	3.81, 3.83	3.82	7
060	3.63	3.63	3
$3\bar{4}0$, 131	3.45	3.45	1
420, $2\bar{2}1$	3.31, 3.32	3.31	3
051	2.976	2.985	1
510	2.738	2.739	4
530, $4\bar{1}1$	2.601, 2.598	2.608	3
540, 431	2.489, 2.490	2.493	1
190	2.400	2.394	1
600	2.290	2.292	1
620, $5\bar{1}1$	2.257, 2.259	2.258	1

+Not fully resolved from the 11.81Å peak. This peak may correspond to an amorphous halo observed on all film-recorded diffraction patterns.

*All peak positions were determined by a peak-search program. The 8.9Å peak was not located thus. The reading was made visually and is therefore not as accurate as other values.

Except for the two peaks identified above, the least-squares procedure used the hk0 data with d-spacings greater than 3.0Å.

Table III

Raman Band Assignments for Si Backbone Vibrations

No.	Frequency cm^{-1}	I_{YY}	I_{YX}	I_{ZY}	I_{ZX}	Assignment	Symmetry Species
2	372	244	42	9	2	Si-Si backbone, ν_s(Si-Si)	A_g
4	458	16	27	16	3	Si-Si backbone, ν_{as}(Si-Si)	B_{2g} or B_{3g}
5	467	120	20	5	1	Si-Si backbone; non-trans conformers	
7	494	212	51	20	4		
9	689.5	953	110	41	12	Si-C symmetric str., ν_s(Si-C)	A_g

Table IV

Symmetry Analysis of the Planar Zig Zag Conformation of PDHS

Polarization[a] Experiment	Symmetry Species A_g	B_{1g}	B_{2g}	B_{3g}
X(YY)Z	α_{zz}^2	0	0	0
X(ZY)Z	0	0	$\frac{1}{2}\ \alpha_{zx}^2$	$\frac{1}{2}\ \alpha_{yz}^2$
X(ZX)Z	$\frac{1}{8}\left(\alpha_{xx}^2 - \alpha_{yy}^2\right)$	$\frac{1}{2}\ \alpha_{xy}^2$	0	0

[a]Porto notation: see text and Ref. 7.

Table V

Raman Bands Assigned to the Hexyl Side Chain

No.	Frequency cm^{-1}	I_{YY}	I_{YX}	I_{ZY}	I_{ZX}	Ref. 8	Ref. 9	Assignment	Symmetry Species+
19	1059	0	6	5	11	1063	1063	$\nu_{as}(CC)$	b_{2g} (b_{2g})
22	1175	124	24	10	13	1170	1181	$r(CH_2)$	b_{1g} ($a_g + b_{2g}$)
23	1244	26	3	1	2		1265		
24	1297	6	25	13	7	1296	1300	$\gamma(CH_2)$	b_{3g} (b_{3g})
25	1414	8	2	1	2	1418			a_g (a_g)
26	1443	18	6	3	2	1445	1440	overtone	a_g (a_g)
27	1453	24	10	7	11	1453	1454	$\delta(CH_2)$	a_g (a_g)
28	1461	5	5	3	11	1456	1467		b_{1g} (b_{2g})

*ν_{as} - asymmetric stretch; ν_s-symmetric stretch; r-rock; γ-twist; δ-bend.

+Symmetry species in parentheses corresponds to assigments made in Ref. 9

REFERENCES

1. For a review see: Proc. Int. Conf. on the Physics and Chemistry of Low-dimensional Synthetic Metals, *Mol. Cryst. Liq. Cryst.* 117 (1985).
2. H. Kuzmany, M. Mehring and S. Roth, "Electronic Properties of Polymers and Related Compounds," *Springer Series in Solid State Sciences 63* (Springer Verlag, Berlin Heidelberg, New York, Tokyo, 1985).
3. R. D. Miller, D. Hofer, J. F. Rabolt and G. N. Fickes, *J. Am. Chem. Soc.* **107**, 2172 (1985).
4. J. F. Rabolt, D. Hofer, R. D. Miller and G. N. Fickes, *Macromolecules* **19**, 611 (1986).
5. J. R. Damewood, Jr., *Macromolecules* **1793**, 18 (1985).
6. P. Trefonas, P. I. Durovich, X. M. Zhang, R. West, R. D. Miller and D. Hofer, *J. Polym. Sci. Polym. Lett. Ed.* **21**, 819, (1983).
7. T. C. Damen, S. P. S. Porto and B. Tell, *Phys. Rev.* **142**, 570 (1966).
8. M. J. Gall, P. J. Hendra, C. J. Peacock, M. E. A. Cudby and H. A. Willis, *Spectrochimica Acta* **28A**, 1485 (1972).
9. R. F. Schaufele, *J. Chem. Phys.* **49**, 4168 (1968).
10. H. Bock, W. Ensslin, F. Fehler and R. Freund, *J. Am. Chem. Soc.* **98**, 668 (1976).
11. H. Kuzmany, P. R. Surjan and M. Kertesz, *Solid State Communic.* **48**, 243 (1983).
12. L. F. Brough and R. West, *J. Am. Chem. Soc.* **103**, 3049 (1981).
13. K. Hassler, *Spectrochim. Acta* **37A**, 541 (1981).
14. K. Hassler, *Spectrochim. Acta* **40A**, 775 (1984).
15. R. G. Snyder, *J. Mol. Spectrosc.* **37**, 353 (1971).
16. N. E. Schlotter and J. F. Rabolt, *Polymer* **25**, 165 (1984).
17. R. D. Miller, private communication.

18. H. Kuzmany, R. D. Miller and J. F. Rabolt, to be published.

19. B. L. Farmer, J. F. Rabolt an R. D. Miller, to be published.

20. R. G. Snyder, S. L. Hsu and S. Krimm, *Spectrochimica Acta* **34A**, 395 (1978).

FIGURE CAPTIONS

Figure 1. Geometrical relationship between molecular and laboratory axes used in recording Raman spectra of ultradrawn films.

Figure 2. Raman spectra for unoriented (A) and oriented (B,C,D) PDHS as excited with green and blue laser light, respectively. Each scattering geometry is labeled according to Porto notation, as indicated in the text.

Figure 3. Observed splitting for the Raman bands # 11, 12, 16 and 17 using a spectral resolution of 1.5 cm^{-1}.

Figure 4. Comparison of Raman spectra for natural and ^{13}C substituted PDHS as excited with the laser line at 4880Å.

Figure 5. Polarized Raman spectra for bands # 18, 19 and 24. The relative intensities are directly comparable.

Figure 6. Same as Fig. 2 but for the CH-stretching region.

Figure 7. Fiber diffraction pattern of oriented PDHS obtained at room temperature. Arrow indicates draw direction.

Figure 8. Phase transition of PDHS as observed in the UV-Vis region at various temperatures between 17°C and 39°C and after returning the temperature to 17°C.

Figure 9. Raman spectra of PDHS as studied at various temperatures between 17°C and 39°C and after returning the temperature to 17°C.

Figure 10. Resonance Raman scattering in the low frequency region of PDHS. All spectra have been "normalized" to their ν^4 scattering factor.

Figure 11. Integrated intensities I(T)/I(17) in relative units for two Raman bands during a temperature cycle. I(T) - integrated intensity at temperature, T; I(17) - integrated intensity at 17°C.

Figure 12. Arrangement of the silicon backbone and the hexyl side chains for an orthogonal geometry. The distances of the atoms are scaled according to standard bond lengths and bond angles.

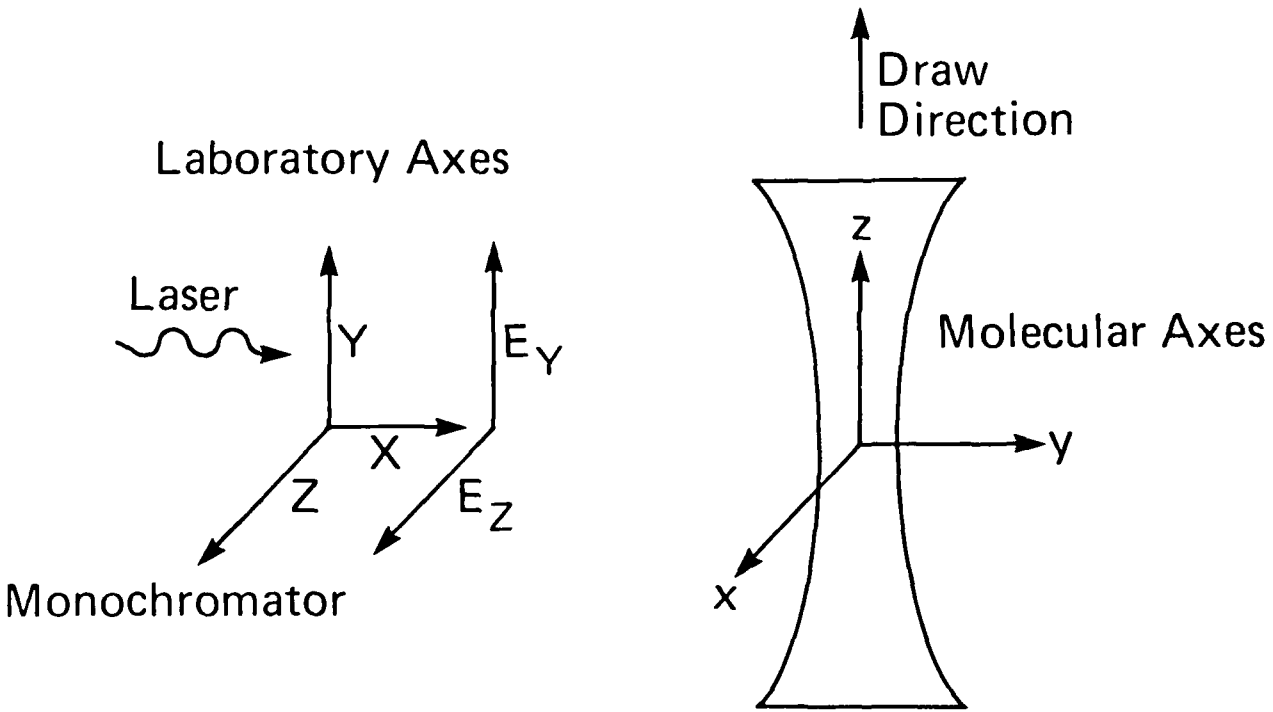
Laboratory Axes
Laser
Y
E_Y
X
Z
E_Z
Monochromator
Draw
Direction
z
Molecular Axes
y
x

Fig. 1

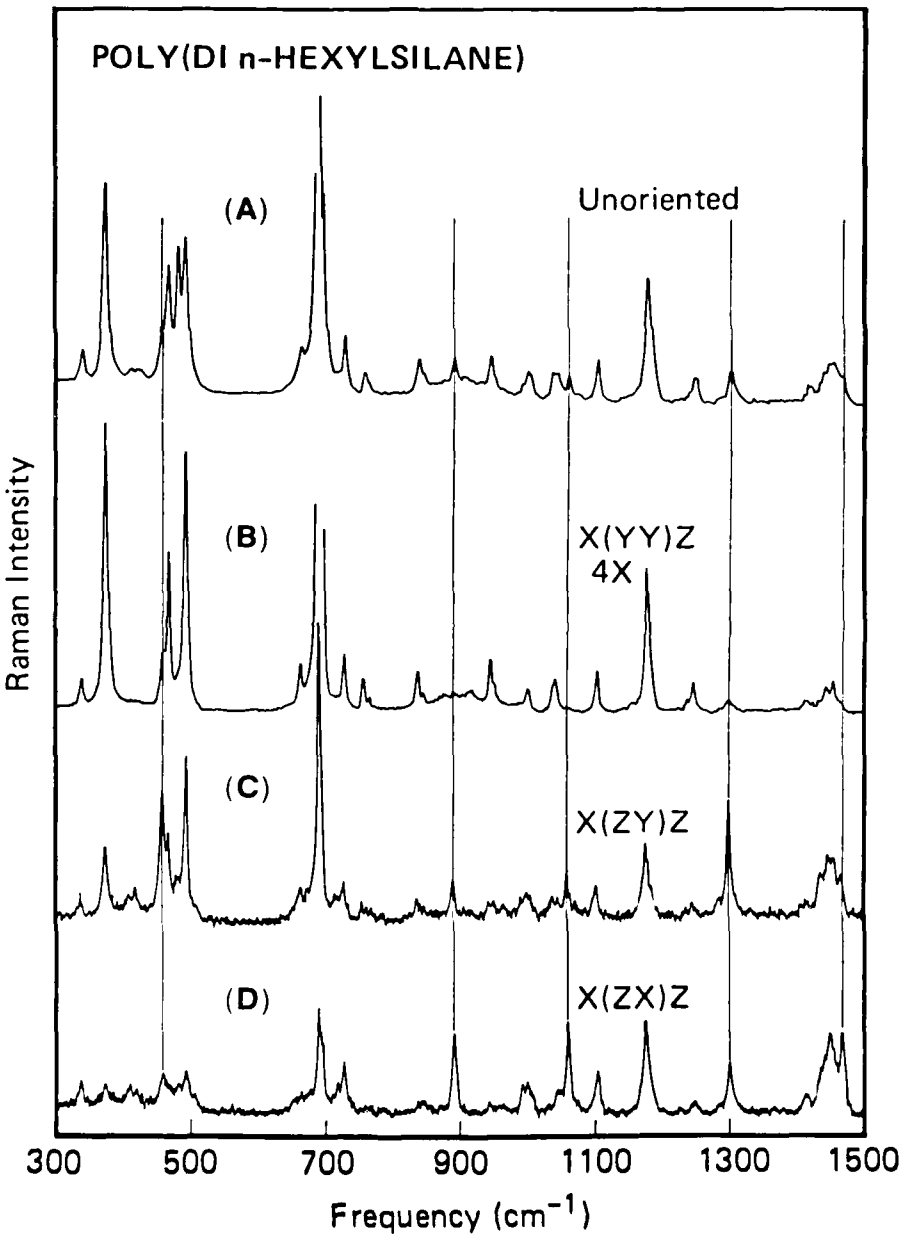
POLY(DI n-HEXYLSILANE)
(A)
Unoriented
(B)
X(YY)Z
4X
(C)
X(ZY)Z
(D)
X(ZX)Z
Raman Intensity
300
500
700
900
1100
1300
1500
Frequency (cm^{-1})

Fig. 2

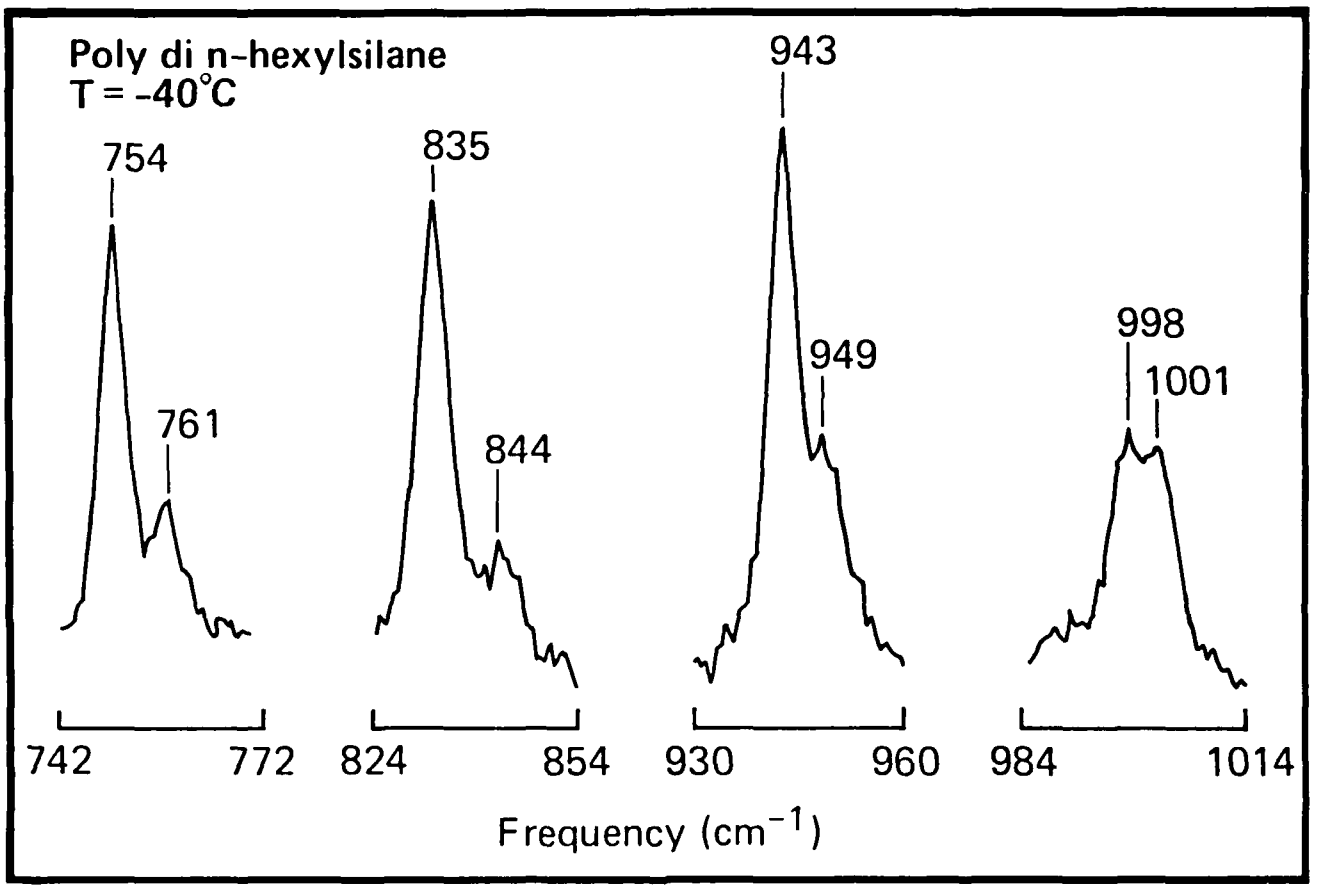
Poly di n-hexylsilane
T = -40°C
754
761
835
844
943
949
998
1001
742
772
824
854
930
960
984
1014
Frequency (cm^{-1})

Fig. 3

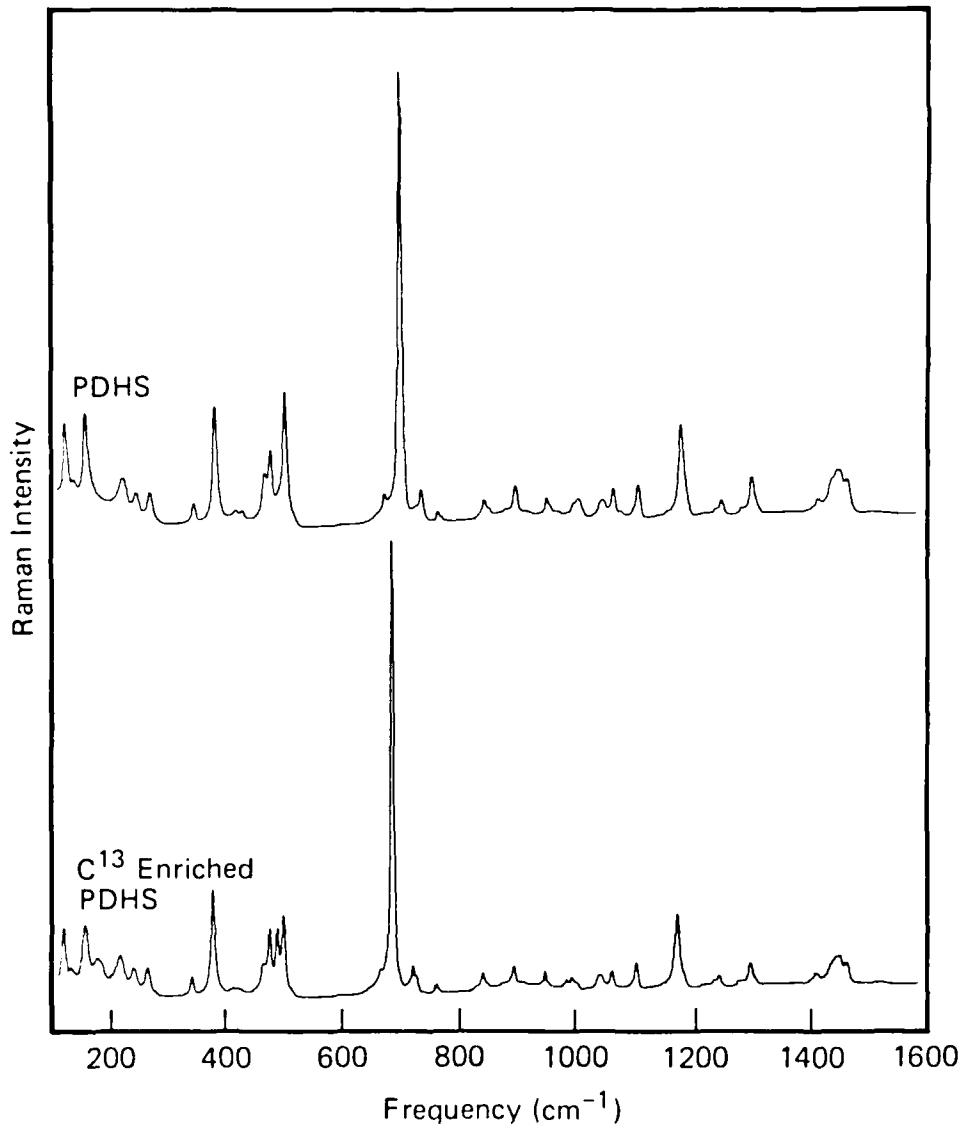
PDHS
C13 Enriched
PDHS
Raman Intensity
200
400
600
800
1000
1200
1400
1600
Frequency (cm-1)

Fig. 4

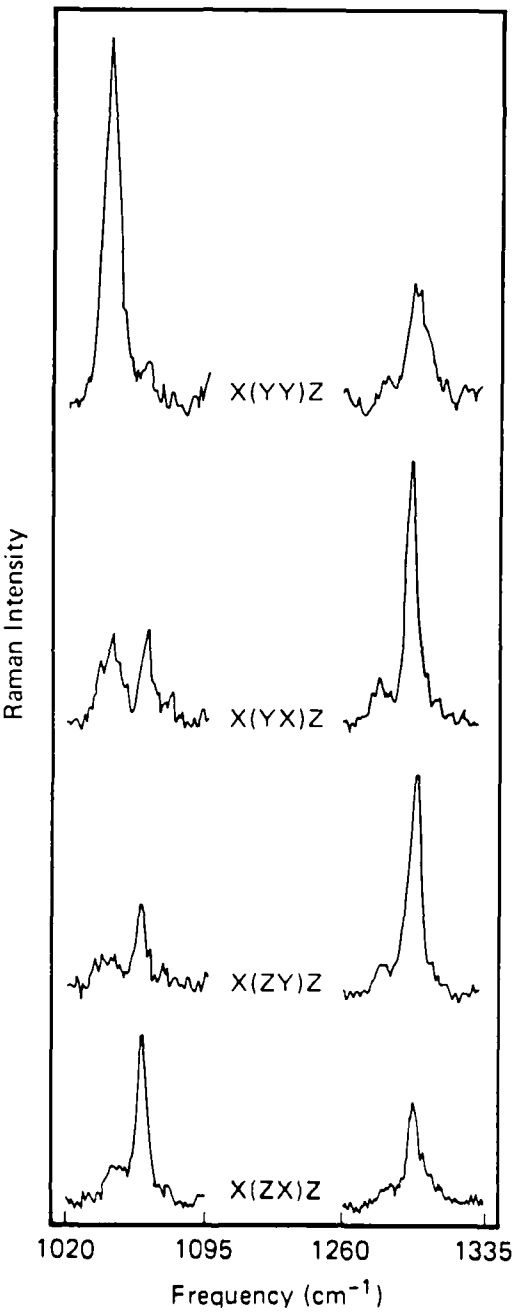
Raman Intensity
X(YY)Z
X(YX)Z
X(ZY)Z
X(ZX)Z
1020
1095
1260
1335
Frequency (cm^{-1})

Fig. 5

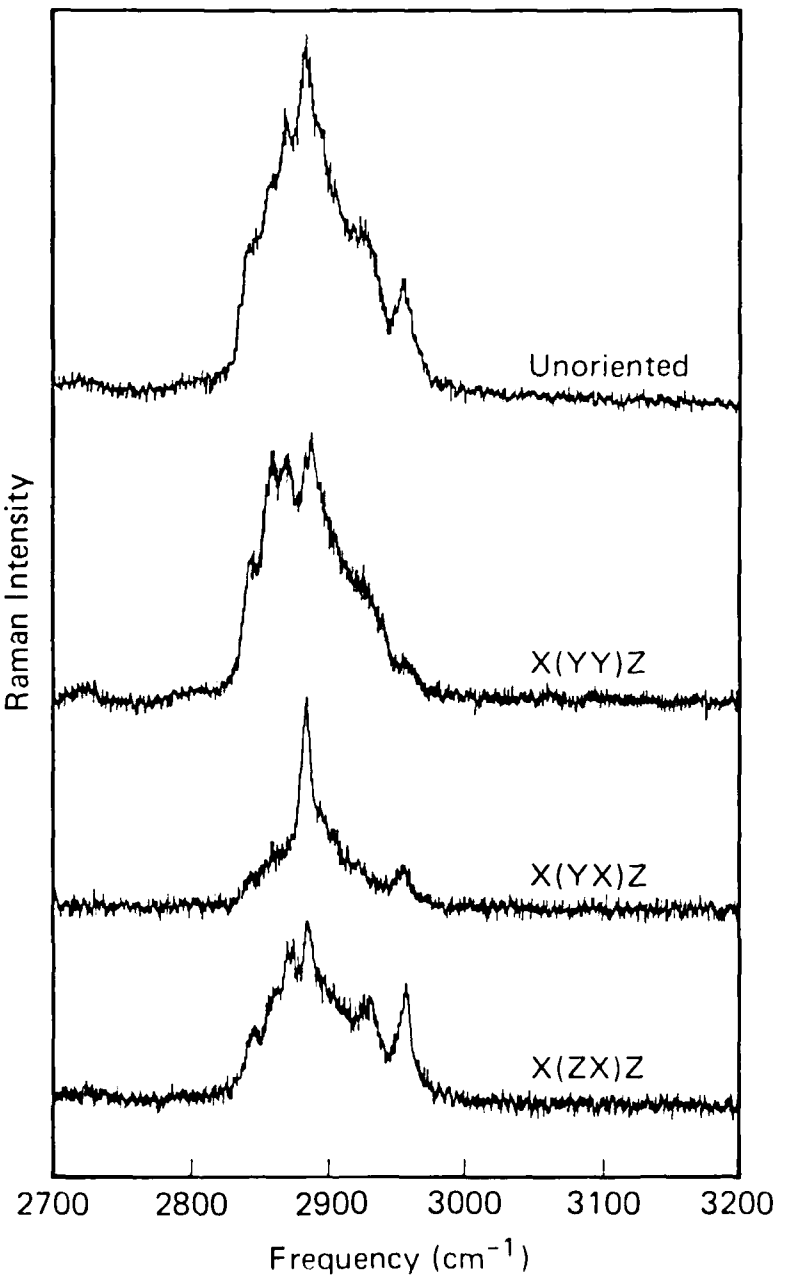
Unoriented
X(YY)Z
X(YX)Z
X(ZX)Z
Raman Intensity
2700
2800
2900
3000
3100
3200
Frequency (cm^{-1})

Fig 6

Oriented Poly(di n-hexylsilane)

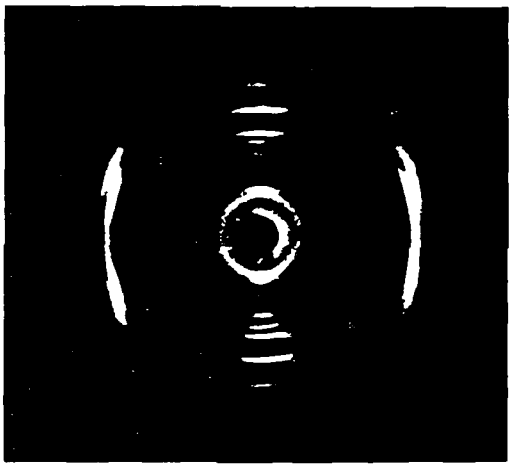

Draw direction

Fig. 7

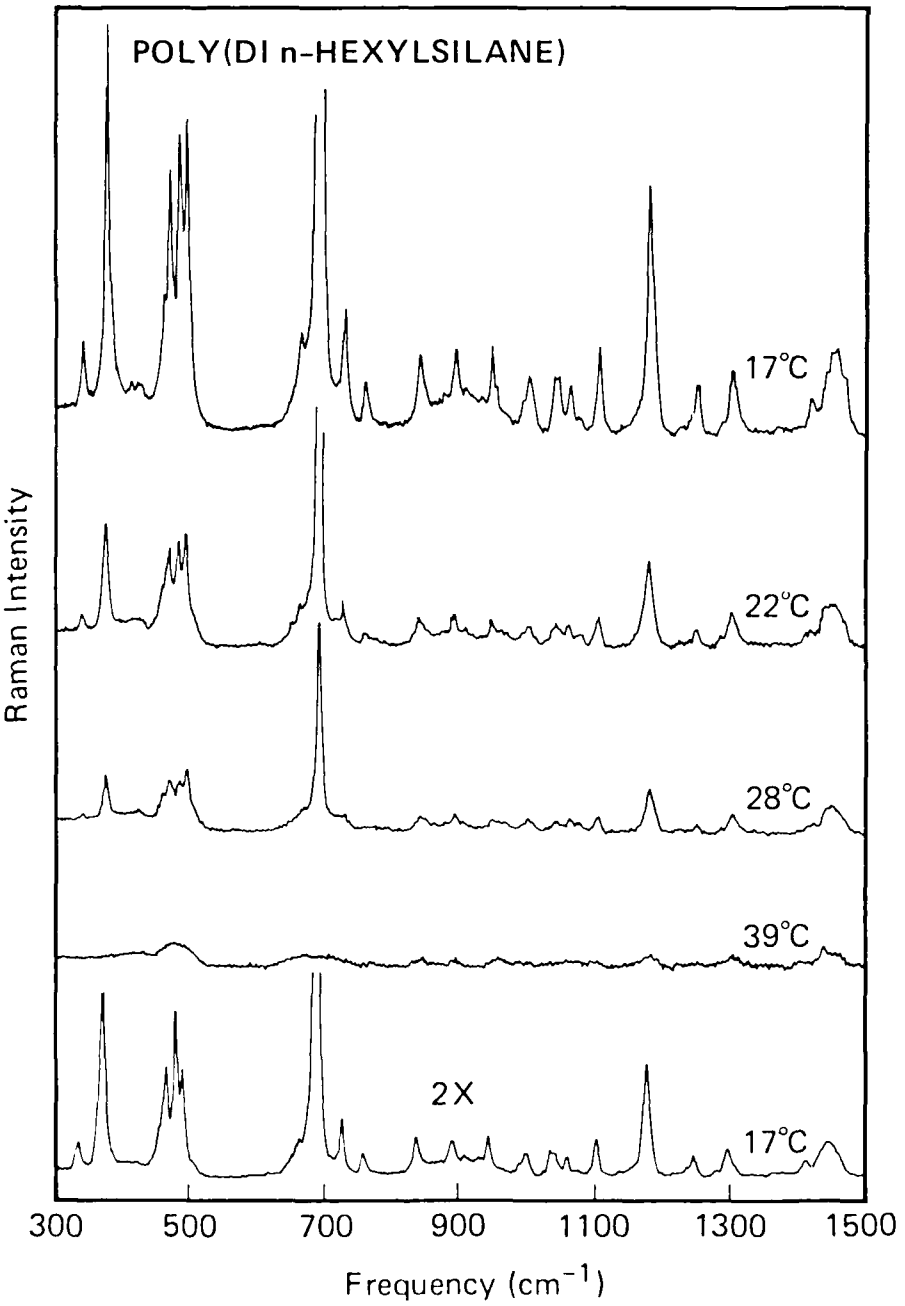
POLY(DI n-HEXYLSILANE)
17°C
22°C
28°C
39°C
2X
17°C
Raman Intensity
300
500
700
900
1100
1300
1500
Frequency (cm^{-1})

Fig. 8

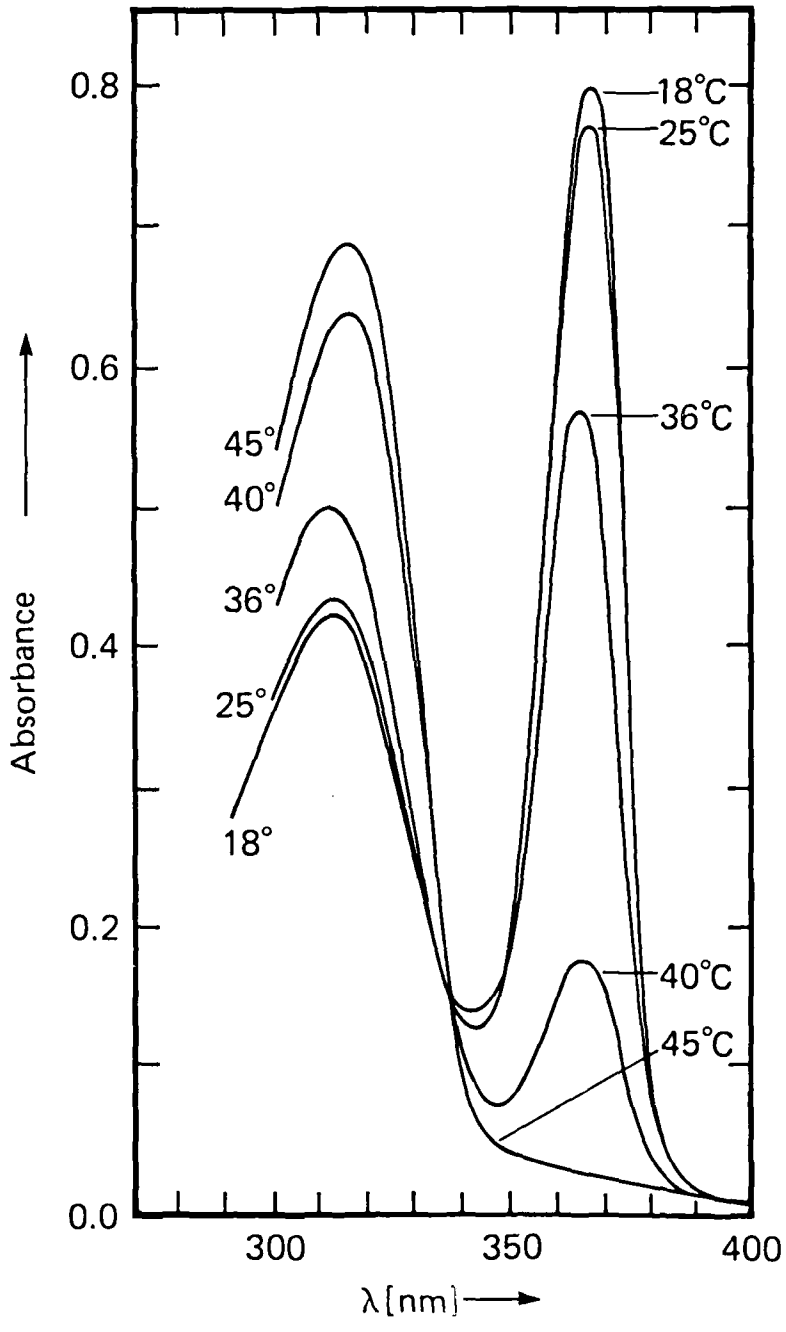
0.8
0.6
0.4
0.2
0.0
Absorbance
300
350
400
λ[nm]
18°C
25°C
36°C
40°C
45°C
45°
40°
36°
25°
18°

Fig. 9

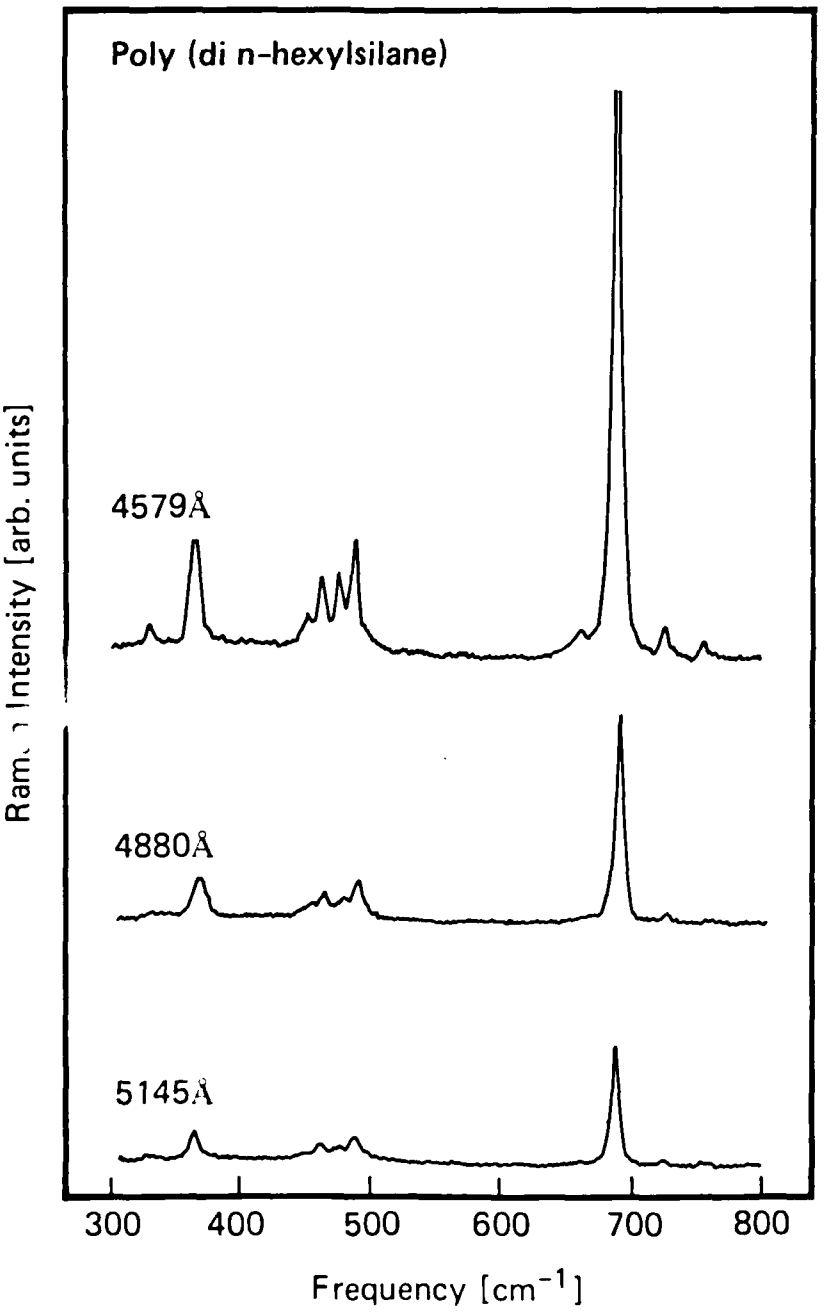
Poly (di n-hexylsilane)
4579Å
4880Å
5145Å
Ram. n Intensity [arb. units]
300
400
500
600
700
800
Frequency [cm^{-1}]

Fig. 1(

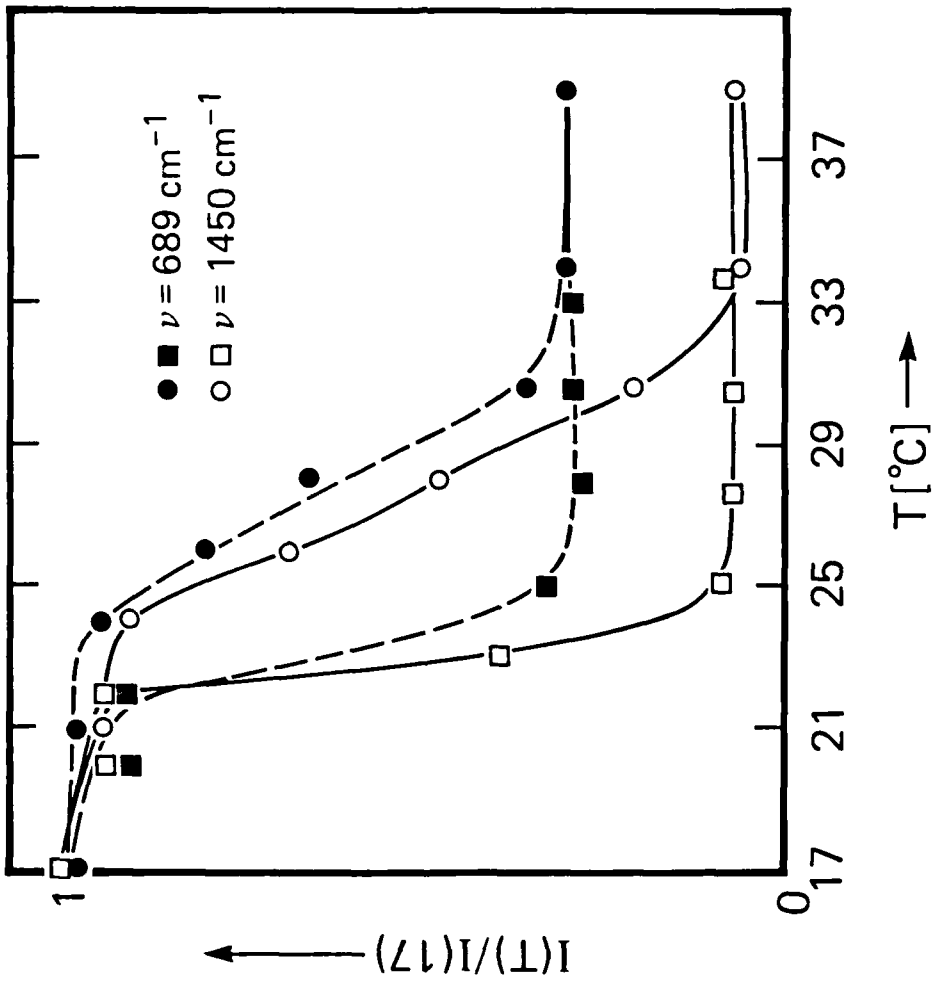

Fig. 1

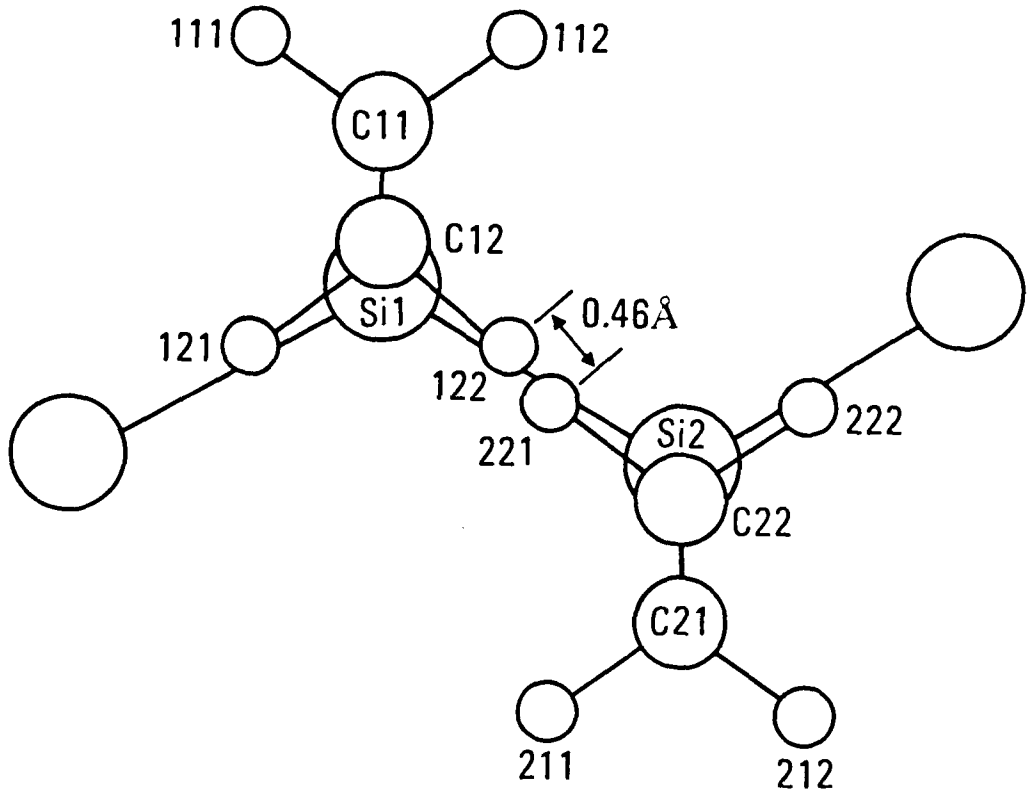

Fig

END

DTIC

9-86